metals

MDPI

Review

Chemical Inhomogeneity from the Atomic to the Macroscale in Multi-Principal Element Alloys: A Review of Mechanical Properties and Deformation Mechanisms

Jiaqi Zhu [1], Dongfeng Li [2], Linli Zhu [3], Xiaoqiao He [1,4,*] and Ligang Sun [2,*]

[1] Department of Architecture and Civil Engineering, City University of Hong Kong, Hong Kong, China
[2] School of Science, Harbin Institute of Technology, Shenzhen 518055, China
[3] Key Laboratory of Soft Machines and Smart Devices of Zhejiang Province, Department of Engineering Mechanics, Zhejiang University, Hangzhou 310027, China
[4] Centre for Advanced Structural Materials, City University of Hong Kong Shenzhen Research Institute, Shenzhen 518057, China
* Correspondence: bcxqhe@email.edu.hk (X.H.); sunligang@hit.edu.cn (L.S.)

Abstract: Due to their compositional complexity and flexibility, multi-principal element alloys (MPEAs) have a wide range of design and application prospects. Many researchers focus on tuning chemical inhomogeneity to improve the overall performance of MPEAs. In this paper, we systematically review the chemical inhomogeneity at different length scales in MPEAs and their impact on the mechanical properties of the alloys, aiming to provide a comprehensive understanding of this topic. Specifically, we summarize chemical short-range order, elemental segregation and some larger-scale chemical inhomogeneity in MPEAs, and briefly discuss their effects on deformation mechanisms. In addition, the chemical inhomogeneity in some other materials is also discussed, providing some new ideas for the design and preparation of high-performance MPEAs. A comprehensive understanding of the effect of chemical inhomogeneity on the mechanical properties and deformation mechanisms of MPEAs should be beneficial for the development of novel alloys with desired macroscopic mechanical properties through rationally tailoring chemical inhomogeneity from atomic to macroscale in MPEAs.

Keywords: multi-principal element alloys; chemical inhomogeneity; chemical short-range order; mechanical properties

Citation: Zhu, J.; Li, D.; Zhu, L.; He, X.; Sun, L. Chemical Inhomogeneity from the Atomic to the Macroscale in Multi-Principal Element Alloys: A Review of Mechanical Properties and Deformation Mechanisms. *Metals* **2023**, *13*, 594. https://doi.org/10.3390/met13030594

Academic Editor: Marek Smaga

Received: 21 February 2023
Revised: 7 March 2023
Accepted: 9 March 2023
Published: 15 March 2023

1. Introduction

Multi-principal element alloys (MPEAs), such as high-/medium-entropy alloys (HEAs/MEAs), as a new class of multi-principal metallic materials, have attracted great attention due to the discovery of their excellent properties. It has been reported that various MPEAs show high strength [1,2], enhanced fracture toughness [3,4], corrosion resistance [5,6], wear resistance [7], impact resistance [8,9], and good thermal stability [10,11]. Most of them can be attribute to the advanced strategies of nanostructure design to improve mechanical properties of conventional metals [12], which have been proved to be effective for MPEAs as well. For example, the rational design of nanotwinned and hierarchical nanotwinned structures [13–16] can not only strengthen and/or achieve ductilization of conventional materials [17–20], but also tailor their deformation and failure modes [21–24]. Owing to the excellent twinning ability for most MPEAs, twinning-induced optimization of their mechanical properties has been widely reported. More importantly, the unique multi-principal nature of MPEAs has inspired researchers to explore the broad constituent space, in addition to utilizing nanostructure-based reinforcement mechanisms, causing MPEA to have greater potential in practical applications.

MPEA solid solutions were initially considered to be a random arrangement of different atoms in the corresponding lattice sites, but several experiments and calculations have

confirmed the existence of compositional inhomogeneity [25,26]. Some recent studies have shown that chemical short-range order (CSRO) is ubiquitous in alloys due to the atomic size mismatch and the interaction between elements using experimental and simulation methods [27–31]. Theoretical or atomic simulations have also demonstrated that CSRO can enhance the energy barrier for dislocation activation and motion, thereby motivating more and more studies on compositional inhomogeneity at different length scales [32]. It has been proved by atomic simulations that CSRO can increase the critical shear stress of dislocation nucleation, decrease the twinning tendency, and promote the formation of stacking fault networks, which can block dislocations [33]. Tang et al. suggested that the interaction between dislocation and chemical medium-range order (CMRO) could significantly improve the yield strength and work hardening rate of the CoCrNi MEA during initial plastic deformation [34]. Theoretically, local chemical order (LCO) and chemical inhomogeneity exist in various kinds of MPEAs, which can play a significant role in tuning the mechanical properties of alloys [35–38]. Actually, there are multiple levels of compositional inhomogeneity exist in MPEAs, including atomic-scale CSRO, nanoscale chemical fluctuations, and centimeter- or even macroscopic-scale chemical fluctuations.

It is worth noting that local microstructure changes or phase transitions may be caused by fluctuations in concentration with sufficiently large wavelengths, resulting in the formation of dual-phase or multiphase MPEAs with nanostructured heterogeneities, which can also be considered a kind of compositional inhomogeneity [39]. The high strength of MPEAs is attributed to the lattice distortion and solid solution strengthening caused by high configurational entropy. In addition, the strength of MPEAs can be improved using traditional methods such as grain refinement and secondary phase precipitation strengthening, but it is often subject to the strength–plasticity trade-off. In this case, finding a suitable method to break through the strength–plasticity trade-off is the key to improve the overall performance of alloys. In traditional alloys, the design of the gradient metal or heterostructure is beneficial to some properties of alloys, making them more suitable for practical engineering applications. Inspired by this, realizing the tunability of mechanical properties by tuning the spatial distribution of chemical structures to achieve a heterostructure-like mechanism has become a topic worth exploring. It is worth noting that the influence of compositional inhomogeneity on the mechanical properties of alloys is still controversial. Although many studies have demonstrated the positive impact of compositional inhomogeneity on various aspects of mechanical behaviors, there is still research reporting that plastic deformation behavior and yield stress do not change much as a result of CSRO [40], and compositional inhomogeneity can even result in the deterioration of the strength and ductility of interstitial dual-phase high-entropy alloys [41]. Therefore, it is necessary to objectively analyze and judge the role played by compositional inhomogeneity in achieving the strengthening and ductilization of alloys through reasonable design.

Compositional inhomogeneity can exist in different forms in MPEAs, and no clear classification for inhomogeneity at different length scales is available. In MPEAs, due to the diversity of elements, the variations in the local chemical environments of random solid solutions due to CSRO, segregation, precipitation, or ordered configurations are very complicated [38]. Therefore, it is difficult to study the chemical inhomogeneity either theoretically or experimentally. However, accurate characterization of compositional inhomogeneity is crucial to fully understanding the structure–property relationships in MPEAs. This paper aims to briefly review different kinds of chemical inhomogeneities at different length scales in MPEAs, and their impact on mechanical properties. The impact of CSRO on stacking fault energy (SFE), dislocation nucleation and motion, and strength and plasticity of MPEAs is reviewed. Then, the effect of segregation and larger-scale chemical inhomogeneity on the mechanical properties are discussed. What's more, the chemical inhomogeneity in some other materials is briefly introduced to provide a reference for the design of MPEAs. It is expected that reasonable design of compositional inhomogeneity will allow the properties of alloys to be flexibly tuned, accelerating the development of high-performance MPEAs.

2. Representative Types of Chemical Inhomogeneity

Chemical inhomogeneity mainly manifests itself in the form of local chemical order, compositional fluctuations at different scales of length, and clustering or segregations [42], as shown in Figure 1. The local enthalpy interaction among compositional elements could be considered to be the driving force in the development of apparent LCO. Due to the diversity of elements in MPEAs, the bonding preference between different constituent species will cause LCO and other inhomogeneity. The CSRO in MPEAs is a well-known chemical inhomogeneity [43,44], as shown in Figure 2a. It shows a bonding preference for different elements over a few neighbor shells [36,45], similar to the formation of ordered intermetallic compounds. In comparison, clustering- and segregation-induced inhomogeneity occurs over larger scales (Figure 2b). Compositional fluctuations exist in scales of length ranging from nanometers (Figure 2c) to micrometers (Figure 2d), and even to macroscopic scale (Figure 2e,f). From atomic-scale chemical structure ordering to larger-scale clustering and concentration fluctuations, we collectively refer to "chemical inhomogeneity" at different length scales.

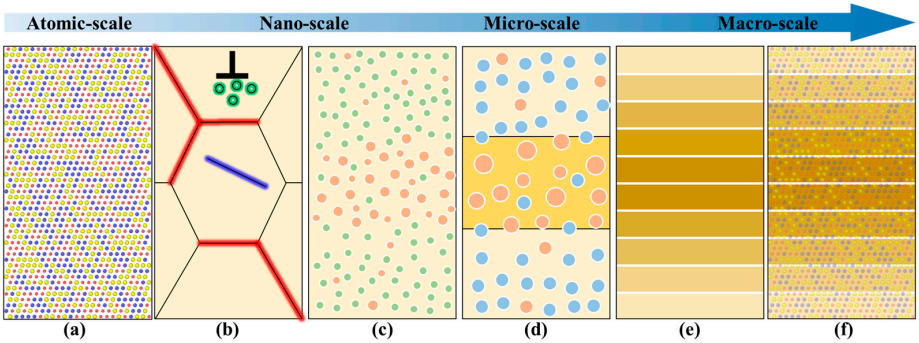

Figure 1. Schematic diagram illustrating different types of chemical inhomogeneity, including (**a**) chemical short-range order, (**b**) segregation of different structures (green, red and blue represent segregation via dislocation, grain boundary and stacking faults, respectively), (**c**) compositional fluctuations, (**d**) compositional fluctuations with phase transition, (**e**) compositional gradient, and (**f**) a combination of compositional gradient and CSRO.

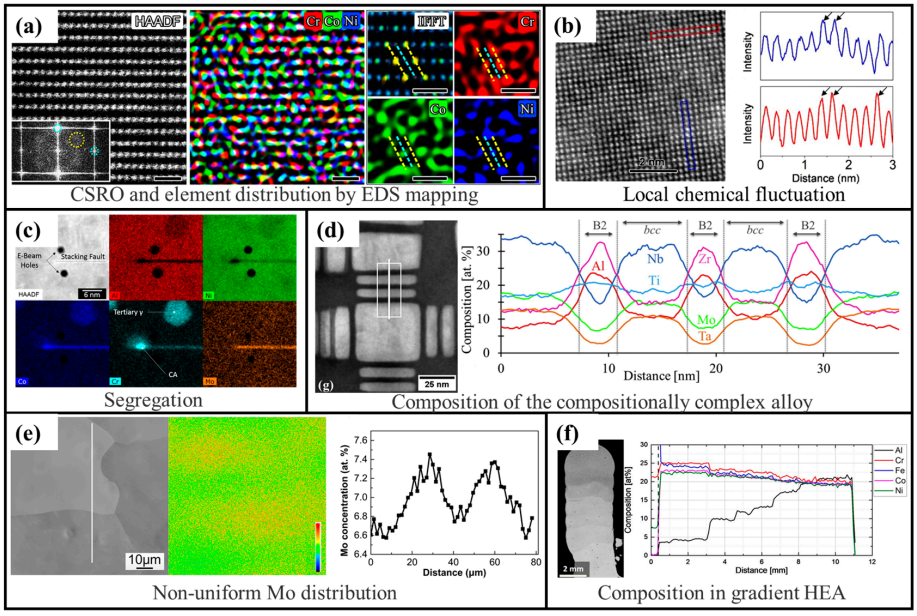

Figure 2. Experimental study on chemical inhomogeneity at different length scales. (**a**) Chemical

short-range order region and element distribution by EDS mapping (Reprinted with permission from Ref. [44]. Copyright 2022, Elsevier); (**b**) nanoscale compositional fluctuation: HAADF−STEM image and the corresponding intensity line profiles of the blue and red squared regions (Reprinted with permission from Ref. [46]. Copyright 2021, Elsevier); (**c**) segregation via stacking faults (Reprinted with permission from Ref. [47]. Copyright 2018, Springer Nature); (**d**) nanoscale compositional fluctuation with phase transition (Reprinted with permission from Ref. [48]. Copyright 2016, Elsevier); (**e**) microscale compositional fluctuations (Reprinted with permission from Ref. [49]. Copyright 2019, Elsevier); (**f**) macroscale compositional gradient in NiCoFeCrAl HEA (Reprinted with permission from Ref. [50]. Copyright 2020, Frontiers).

Experimental methods for the detection of local chemical order in MPEAs have been developed in recent years. Compositional inhomogeneity is first detected in the form of CSRO by extended X-ray absorption fine structure (EXAFS). Laser irradiation is utilized to increase the degree of CSRO, and CSRO is qualitatively determined through data analysis. In order to quantitatively describe the CSRO in MPEAs, more advanced methods are needed to be able to explore the complex atomic occupancy between different elements. High-angle annular dark field scanning transmission electron microscopy (HAADF-STEM) is a method suitable for analyzing the microstructure and performing compositional analysis of atom columns and even single atoms in alloys [51]. Niu et al. identified the existence of non-uniform ordered nano-domains throughout NiFeCrCo random solid solutions using HAADF-STEM measurements. Furthermore, three-dimensional atom probe tomography (3D-APT) supplemented by computational simulations enables the description of CSRO in real-space reconstructed 3D atomic images [52–54]. Recently, Zhang et al. [26] reported the observation of structural features of CSRO in CrCoNi MEA using energy-filtered electron diffraction and HAADF-STEM imaging. It is worth noting that CSRO theoretically only contains a few nearest neighbor atomic layers, but the above studies reveal the local chemical order at the nanometer scale. Therefore, experimental methods can reveal large-scale compositional inhomogeneity (>1 nm), but the characterization of CSRO (<1 nm) remains difficult.

In addition to experimental study, previous theoretical studies [29,31] have demonstrated that CSRO in MPEAs is thermo-dynamically favored and can be designed for the tuning of mechanical properties. Additionally, computational simulation methods are able to provide some predictions regarding the formation of CSRO and its impact on mechanical properties. For example, the hybrid Monte Carlo method and the molecular dynamics simulation method can be used to investigate the properties of MPEAs [55–57]. First-principles calculation combined with Monte Carlo simulation can provide a theoretical model of atomic configuration that can be applied to obtain larger MPEA systems with CSRO [38,58]. A thorough theoretical foundation for related experimental detection is provided by the development of theoretical and modeling approaches, thus also advancing our understanding of the atomic-scale configuration and LCO in MPEAs.

3. Chemical Short-Range Order

3.1. Effect of CSRO on Stacking Fault Energy

SFE in alloys is mainly affected by element type, concentration, distribution, temperature, etc. [59–61]. In traditional crystalline alloys, SFE has an important impact on plastic flow, dislocation movement, deformation twinning, and phase transformation, and the same is true for MPEAs. It can be said that SFE directly or indirectly determines whether dislocation slip, deformation twinning, or close-packed hexagonal (hcp) phase transition will play a dominant role in the plastic deformation process. Investigations of SFE enable researchers to better understand the microscopic mechanisms occurring during plastic deformation. Phase stability and SFE can be tailored by adjusting the element type and concentration in alloys [1,62,63]. Recently, an attempt was made to reduce the SFE of CoCrMnNiFe HEA by controlling the concentration of Co or Cr, so as to tune plastic deformation behavior of twinning-induced plasticity (TWIP) and transformation-induced plasticity (TRIP) [64]. MPEAs possess numerous components and complex chemical struc-

tures, which inevitably produce different degrees of CSRO during the preparation process. It has been reported [31] that SFE in alloys is quantitatively related to the degree of CSRO, increasing with increasing degrees of CSRO. Inhomogeneous distribution of local SFE may affect the plastic deformation mechanism through affecting dislocation slip, deformation twinning and phase transformation. Changing the LCO can significantly alter the preference between face-centered cubic (fcc) and hcp phases [31]. For random solid solutions of CrCoNi MEA in the ground state, the hcp phase is energetically favored [31,65], as shown in Figure 3. With increasing degree of CSRO, the energy of both phases decreases, but the energy of the fcc phase decreases more rapidly. In some chemically ordered states, the hcp phase is energetically comparable to the fcc phase, and the in situ transition from fcc to hcp can easily occur during plastic deformation, which helps to increase the strain hardening rate of the alloys [66], in turn promoting strength–plasticity synergy. At the same time, the low SFE induced by CSRO is beneficial in promoting the formation of nanotwins and hindering the movement of dislocations, thereby improving the strain hardening rate, defect storage capacity and ductility of MPEAs [67–70]. In addition to SFE, CSRO may also affect the energy of different defects, including dislocations, vacancies, and grain boundaries, thereby affecting the deformation mechanism and macroscopic properties of the alloys. It is worth noting that one of the main approaches to induce CSRO in MPEAs is high-temperature annealing, by means of which the degree of CSRO can be tailored by controlling the method of heat treatment. Although there are still some challenges regarding the quantitative experimental observation of CSRO, the rapid development of advanced scanning electron microscope technology is gradually breaking through the difficulties, making it possible to better describe CSRO in MPEAs.

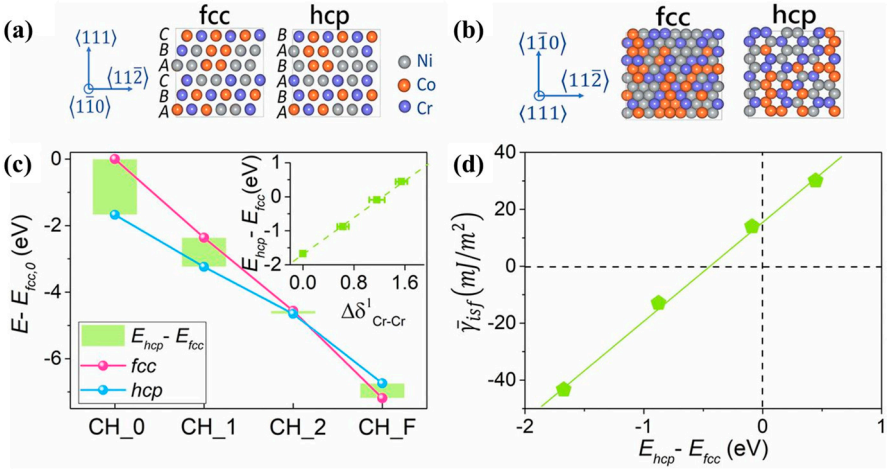

Figure 3. Energies of fcc and hcp structures in NiCoCr solid−solution alloys. (**a**,**b**) Side and top view of atomic configurations. (**c**) Relative energy difference for fcc and hcp phases at various degrees of LCO. (**d**) Correlation between average SFE $\overline{\gamma}_{isf}$ and energy difference for fcc and hcp phases ($E_{hcp} - E_{fcc}$) (Reprinted with permission from Ref. [31]. Copyright 2018, PNAS).

3.2. Effect of CSRO on Dislocation Nucleation and Growth

The physical essence of solid solution strengthening of MPEAs is the elastic interaction between lattice dislocations and solute atoms [71,72], which reduces the lattice deformation and internal stress caused by dislocation nucleation and growth, and increases the resistance of dislocation movement and the difficulty of deformation, so as to achieve a strengthening effect. Other strengthening methods include those involving nanoparticles, precipitation, dual-phase structures, multi-layer structures, etc. The majority of these techniques work to strengthen alloys by limiting the mobility of dislocations, but they do not take into account the nucleation and growth of dislocations, which are the primary determinants of an alloy's elastic properties and mechanical strength. Through nanoindentation simulations, Yang et al. [73] reported that the nucleation force of the first Shockley partial

dislocation within CoCrNi MEA with CSRO was 55% larger than the random solid solution, proving that the MEA with CSRO showed stronger resistance to dislocation nucleation. They suggested that CSRO effectively enhance the hardness of the materials, and this enhancement increased with increasing degree of CSRO, as shown in Figure 4. Ma et al. [74] reported that CSRO could increase the energy barrier of dislocation nucleation and improve the resistance of dislocation cross-slip. Zhao et al. [75] conducted spherical tip nanoindentation experiments on HEAs with an fcc structure. They proposed that a higher degree of CSRO might be attained by managing high-temperature annealing, which would increase the stress needed for uniform dislocation nucleation and thus achieve strengthening of MPEAs. All of these studies suggest that the existence of CSRO can increase the difficulty of dislocation nucleation. In alloys with CSRO, dislocation nucleation, growth and slip need to overcome the energy required to break favorable bonds [76]. Therefore, a higher critical resolved shear stress is required for dislocation nucleation compared with in random solid solutions, which is an important reason for the increase in yield stress. LCO can further enhance the "cocktail strengthening" effect in MPEAs by changing the activation energy barrier of dislocation-mediated plasticity to achieve strengthening and hardening [77].

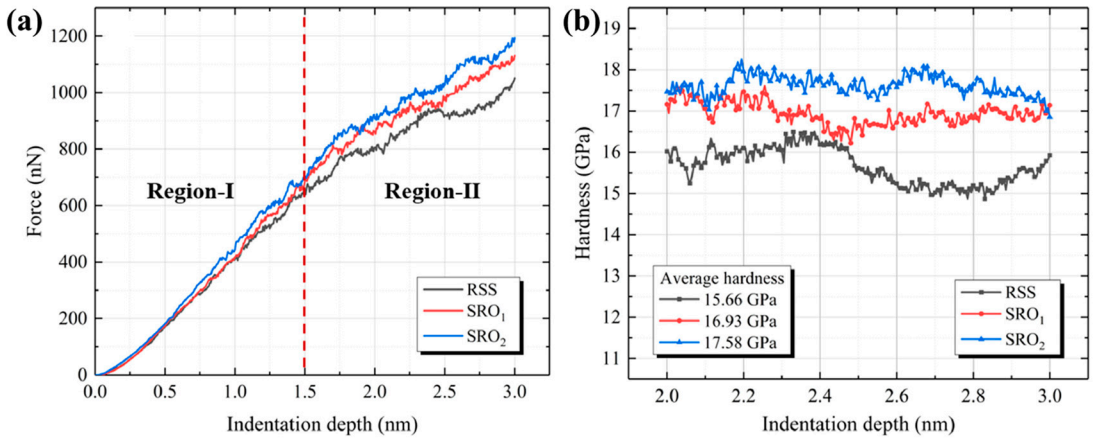

Figure 4. Effect of CSRO on the hardness of alloys. (**a**) Force–indentation depth and (**b**) hardness–indentation depth curves for different structure models (Reprinted with permission from Ref. [73]. Copyright 2022, Elsevier).

3.3. Effect of CSRO on Strength and Plasticity

The fluctuation of SFE induced by CSRO or other compositional undulations [78] can enhance the tortuosity of the dislocation path, which plays a role in dislocation pinning, thereby improving the strength of alloys [79,80]. CSRO can change the energy distribution in the alloys and increase the local potential energy barrier. As shown in Figure 5, by comparing the effective barrier and the resulting strength of NiCoCr alloys with different degrees of CSRO, it can be found that the samples with stronger CSRO will show a greater barrier to dislocation slip. Simultaneously, the increase in activation shear stress clearly indicates the significant strengthening induced by CSRO [32]. In addition, due to the change in the local energy landscape, the original uniform arrangement of atoms and the minimum energy path of dislocation movement are locally changed, resulting in jerky dislocation lines and rough stacking fault belts [81], as shown in Figure 6. This causes the dislocations to move forward non-uniformly, thereby increasing the dislocation slip resistance, and thus leading to increased strength of the alloy.

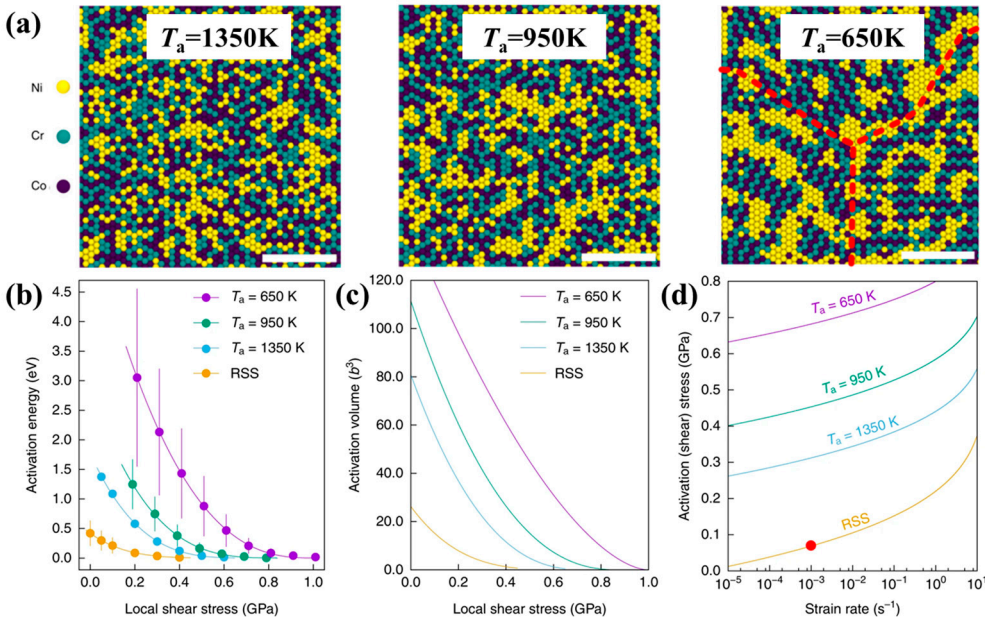

Figure 5. CSRO-induced strengthening (Reprinted with permission from Ref. [32]. Copyright 2019, Springer Nature). (**a**) Configurations of LCO at different annealing temperatures. The red dashed lines indicate the cobalt–chromium (Co–Cr) domain boundaries. (**b**) Average activation barriers. (**c**) Average activation volume. (**d**) Average activation (shear) stress.

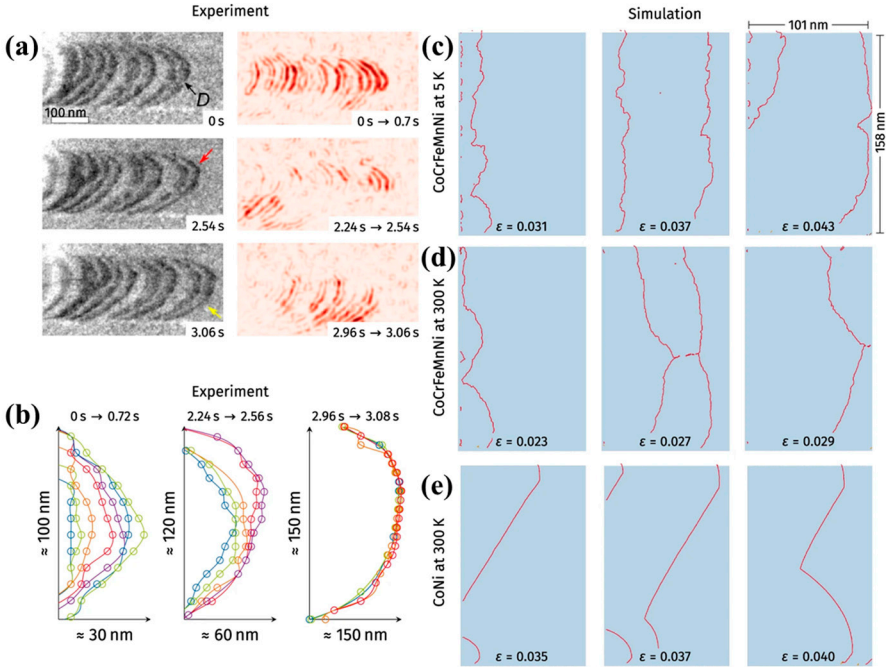

Figure 6. Jerky dislocation motion (Reprinted with permission from Ref. [81]. Copyright 2022, Springer Nature). (**a**) A series of TEM snapshots and schematic figures showing a sequence of gliding Shockley partial dislocations. Black arrow represents dislocation lines, red and yellow arrows denote the movement of dislocations captured at denoted time intervals. (**b**) Extracted dislocation line of the leading partial dislocation which show jerky glide motion because some segments get pinned during glide. (**c**,**d**) Atomistic simulation results with strong pinning of dislocations and (**e**) weak pinning of dislocations. The presence of CSRO in CoCrFeMnNi alloys results in jerky dislocation motion while the CoNi alloy with weak pinning shows almost ideally straight dislocation lines.

As shown in Figure 7, CSRO has a significant influence on the strength and plasticity of MPEAs. Due to the resistance from CSRO when the stacking fault propagates, the generation and development of deformation twins become easier, which improves the plastic deformation ability of the alloy. A previous study [82] suggested that the occurrence of deformation twins is an important means for achieving strength–plasticity synergy in many kinds of MPEAs. Furthermore, Sun et al. [83] stated that the existence of CSRO may change the critical shear stress of each slip plane, leading to the activation and deformation of the sub-slip plane and improving the plasticity of the alloy. The non-uniform distribution of local elements caused by CSRO increases the possibility of interaction between different elements, promoting the activation of cross slip and the change in the dislocation slip path [84,85]. Therefore, the plastic flow in the alloys can be diffused to multiple planes through LCO. During the dislocation movement, some atomic planes may lose their original LCO and rebuild a new LCO, which will obviously affect flow stress during the plastic deformation stage [32]. However, interestingly, the effect of CSRO on the mechanical properties of MPEAs remains controversial. Although many studies have suggested that CSRO can increase the strength and plasticity of MPEAs, Yin et al. [86] examined the yield strength of CoCrNi MEA with CSRO and argued that CSRO has a negligible effect on the strength of this kind of MEA. Therefore, the high strength of NiCoCr is not necessarily due to CSRO, but rather the volume and elastic misfit of MPEAs. According to current knowledge, the formation of CSRO has a very close relationship with the heat treatment process; therefore, we speculate that the differences between individual studies are likely to come from different processing methods.

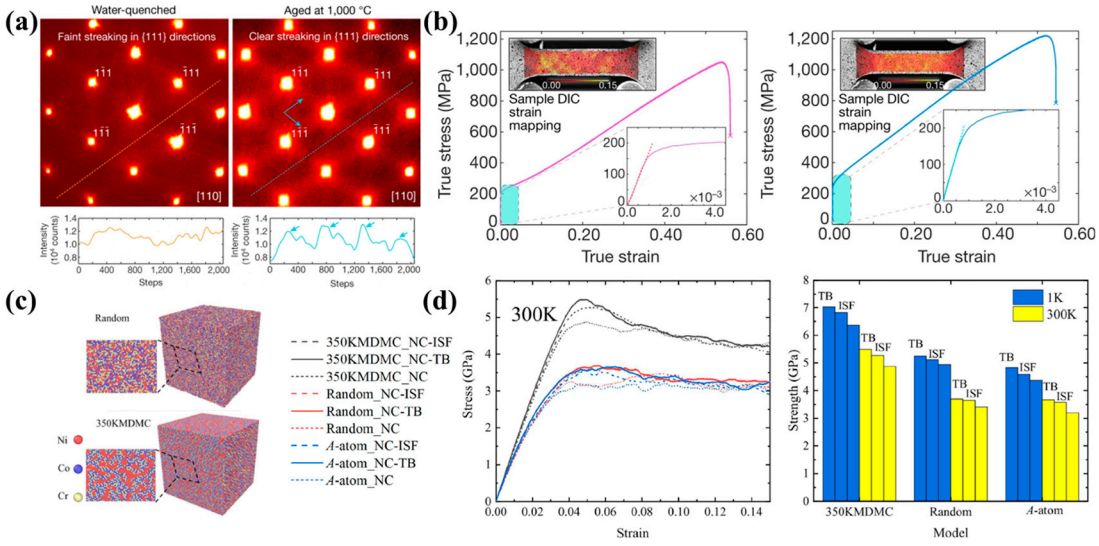

Figure 7. Effect of CSRO on the mechanical properties of MPEAs. (**a**) Main panels, energy-filtered diffraction patterns for water-quenched and aged samples, respectively. Plot below shows intensity measured along the diagonal line in the main panel (Reprinted with permission from Ref. [26]. Copyright 2020, Springer Nature). (**b**) Tensile stress–strain curves of a water-quenched sample (left) and an aged sample (right), respectively. Lower insets represent the elastic portions of the curves (Reprinted with permission from Ref. [26]. Copyright 2020, Springer Nature). The aged samples with strong CSRO shows a better performance. (**c**) Atomic configurations of MPEAs with and without CSRO (Reprinted with permission from Ref. [36]. Copyright 2020, Elsevier). (**d**) Stress–strain relation and the strength of CoCrNi alloys with the effect of CSRO (Reprinted with permission from Ref. [36]. Copyright 2020, Elsevier). The results show that the presence of CSRO greatly improves the strength and plasticity of CoCrNi MEA.

4. Segregation-Induced Chemical Inhomogeneity

In crystalline solids, through chemical and mechanical interactions between atoms and defects, solute atoms tend to segregate into extended defects, such as dislocations [87–89],

grain boundaries [90–101], and other defect structures. Compared to perfect bulk crystals, one of the characteristics of dislocations and grain boundaries is that the presence of crystal defects increases the Gibbs energy. Systems containing dislocations and grain boundaries tend to reduce this energy in several ways. For example, some alloying elements will be enriched near dislocations (Figure 8a) or grain boundaries (Figure 8b) during the thermodynamic optimization process, which reduces the energy of the system such that a stable state is obtained. Segregation refers to changes in local element concentration caused by the above situation. Kang et al. [89] reported that, due to the high strain energy of dislocations, the effect of configurational entropy on the uniform distribution of atoms decreases significantly. The stronger interactions between atoms with higher size misfits and dislocations encourage the preferred segregation to dislocations in order to reduce the dislocation line energy [102–106], which has a significant effect on dislocation creep behavior. The critical stress imposed by the elastic interactions between segregated solute atoms and dislocations that must be overcome by partial dislocations is much larger than CSRO, leading to the tardiness of dislocation cross-slip and the emergence of wave-like slip behavior [103,107,108]. Additionally, grain boundary and surface segregation can change the interfacial compositional structure, such as the segregation in Cantor alloys [109–112], Cu-Nb alloys [113], Cu-Ag alloys [114], Ni-Ti alloys [115], etc. Wynblatt et al. [109] suggested that the main driving forces for grain boundary segregations are interfacial energy, element interactions, and internal strain energy arising from size misfits. The degree of segregation of different elements will be affected by many factors, such as chemical constituents, interface structures, and grain size. Some studies have suggested that the addition of certain solute atoms to the grain boundary will decrease the grain boundary energy, thus suppressing grain growth [116–118] and enhancing the fracture toughness and strength [115]. Recent studies have shown that the segregation of solute atoms at the grain boundaries can further enhance the strength and hardness of nanocrystalline materials [119–121]. Conversely, grain boundary segregation may embrittle the grain boundaries which makes it more likely to failure [122–124].

Solute atoms also segregate at stacking faults (Figure 8c), a phenomenon commonly known as Suzuki segregation [47,125–131]. Ni-based superalloys, as a critical class of high-temperature-resistant materials, are usually able to achieve excellent high-temperature mechanical properties from coherent fcc γ' precipitates [132,133]. In particular, investigations on the creep properties and microstructure of Ni-based superalloys have attracted much attention. For example, dislocation glide in the γ matrix [134–136] can lead to the formation of dislocation networks around γ' particles [137–140], the dislocation shearing of γ' particles [141–144], etc. Suzuki segregation usually occurs in superlattice intrinsic and extrinsic stacking faults in the γ' particles of MPEAs. Segregation, as one of the manifestations of chemical inhomogeneity, has been the subject of intensive studies with respect to its role in stacking faults and its impact on the mechanical properties on MPEAs. The effect of stacking fault segregation on Ni-based superalloys is mainly reflected in the control of creep properties. Through atomic resolution characterization of the active γ' shearing mechanisms, Smith et al. [128] reported that stacking fault segregation may be key to improving creep strength by slowing the formation and extension of twins. The change in local SFE due to segregation affects the dissociation behavior of dislocations, thereby affecting the dislocation cross-slip and twinning behaviors. Since SFE is dependent on the local compositional distribution [79,145,146], the stacking fault segregation also affects the deformation behavior of MPEAs. Due to the elemental diversity of MPEAs, the segregation tendency of various elements is difficult to predict and cannot be generally applied to all cases. The segregation of different elements near different defects will have different effects on the mechanical properties. Zhao et al. [147] demonstrated that the segregation of Co/Cr in complex stacking faults can improve interfacial stability and plastic deformation capacity. In addition, the segregation of Co at superlattice intrinsic stacking faults is beneficial in increasing work hardening. These studies were focused on the influence of segregation

on the mechanical properties of alloys, providing ideas for the rational composition and structural design of Ni-based alloys and other alloys.

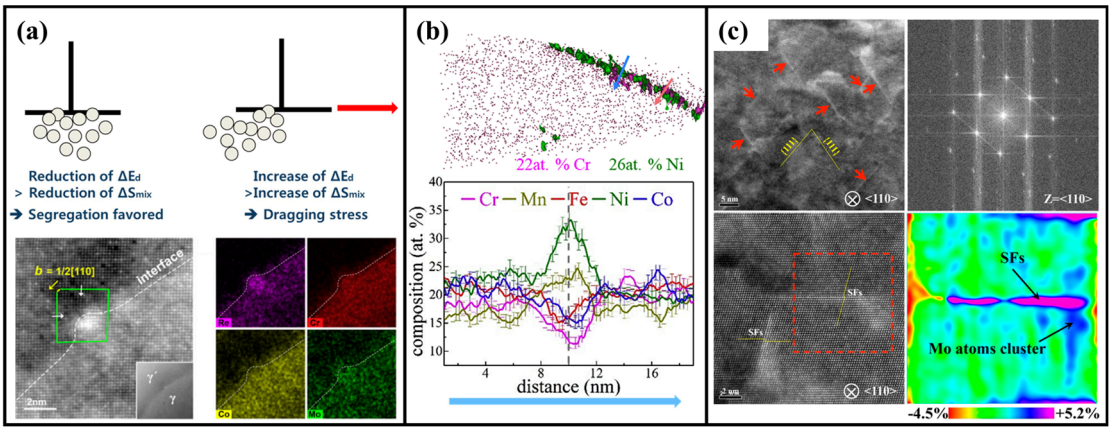

Figure 8. Solute segregation for different structures. (**a**) Hypothetical representations of interaction of atoms with a dislocation and STEM and chemical analysis of interfacial dislocation core structure at the atomic scale. The green square indicates the position of dislocation core. The lower right corner shows the EDS maps showing distribution of elements Re, Cr, Co, and Mo at the dislocation core are (Reprinted with permission from Ref. [87]. Copyright 2018, Elsevier; Reprinted with permission from Ref. [89], Copyright 2018, Taylor & Francis). (**b**) Segregation at grain boundaries along the blue arrow (Reprinted with permission from Ref. [110]. Copyright 2019, Elsevier). (**c**) HAADF−STEM image of Cr20Fe6Co34Ni34Mo6 alloy showing the segregation of Mo to stacking faults. The red arrows represent the stacking faults. The lower right corner shows the elemental distribution in the red square (Reprinted with permission from Ref. [130].Copyright 2019, Taylor & Francis).

5. Chemical Inhomogeneity at Larger Scales of Length

Chemical inhomogeneity in the MPEAs exists at a variety of different scales of length. In addition to CSRO [148] and CMRO [149] at the atomic scale, there is also the inhomogeneity of elemental distribution at the micro-/nanoscale [48,150], or even at the macroscale [151] (Figure 2). In addition to structural heterogeneity [14,152–154], many attempts have been made to achieve tunability of the deformation mechanism through chemical structure design with the purpose of enhancing strength–plasticity synergy. In our previous works, by designing a compositional gradient for every constituent [155], we were able to achieve enhanced tensile strength and plastic deformation capacity in CoCrNi MEA. Obvious strain hardening and plastic strain delocalization were observed in MEA with compositional periodicity and short-range order [156]. In these previous studies, the alloys maintained a single-phase fcc structure despite the presence of chemical inhomogeneity. In larger-scale chemically inhomogeneous alloys, local phase transitions from single-phase solid solutions to dual-phase or even multi-phase solid solutions may occur due to the presence of compositional fluctuations. With a sufficiently large wavelength of compositional fluctuation, local phase transformation will occur inside the alloys. For example, Chen et al. investigated spinodal decomposition-induced compositional heterogeneity and suggested that the formation of the three-dimensional chemical heterostructure through spinodal decomposition effectively impeded dislocation motion and promoted the formation of a high-density dislocation loop [157]. By controlling the inhomogeneity of Mo in (CoCrNi)93Mo7 MEA, a heterostructure with banded precipitates was generated, promoting strength–plasticity synergy [49], as shown in Figure 9. Kuczyk et al. [50] suggested that compositional distribution can be controlled through laser metal deposition to achieve a chemical gradient structure. They proposed a suitable methodology for synthesizing AlCoCrFeNi HEA with a millimeter-scale compositional gradient. The change in microstructure from single-phase to a fine-scaled dual-phase bcc solid solution was detected, and the relationship between

the microstructure and the hardness of the HEA with both uniform and gradated chemical distributions was investigated.

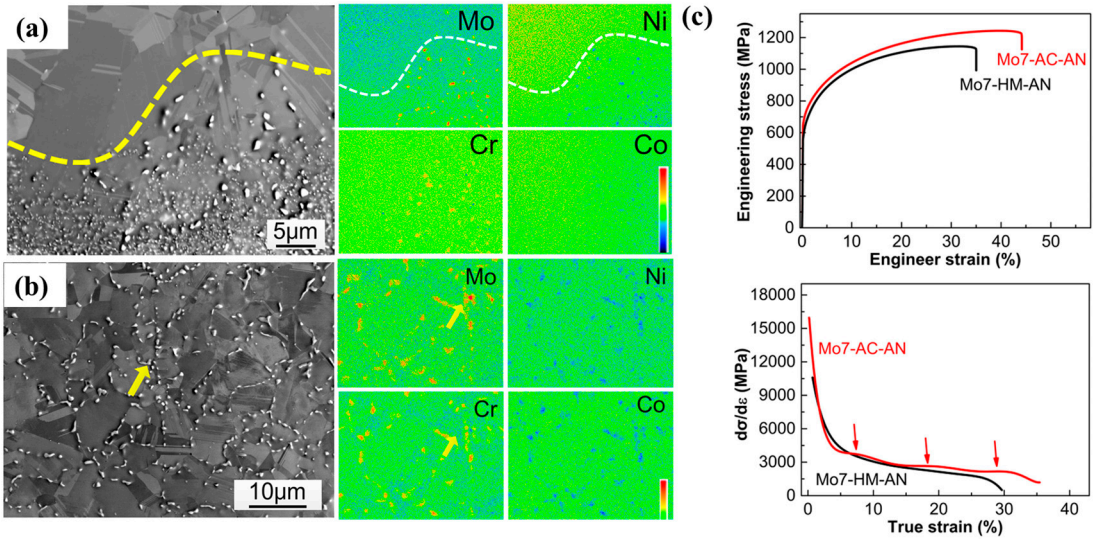

Figure 9. Tensile properties affected by chemical distribution (Reprinted with permission from Ref. [49]. Copyright 2019, Elsevier). (**a**) SEM micrographs and elemental distribution of as–cast (Mo7–AC–AN) and (**b**) homogenized (Mo7–HM–AN) HEAs. (**c**) Engineering stress–strain and work hardening rate curves of the two alloys. The red arrows represent the strain hardening rate platform.

In addition to MPEAs, there have been some studies on controlling the mechanical properties by tuning the compositional distribution in traditional alloys to better realize engineering applications. For example, Wu et al. [158] designed Ti/Ti_3Al ductile and brittle composites by simultaneously controlling the macroscopic lamination structure and microscopic compositional gradient, giving full play to the ability of the structure and chemical design to disperse local strain during deformation. In this way, the plastic flow can be effectively stabilized by strain delocalization to achieve superior mechanical properties. Hofmann et al. [159] performed finite element simulations on an automobile valve stem and demonstrated a reduction in stress by an order of magnitude at the alloy joints with a centimeter-scale compositional gradient. Although these studies are not focused on MPEAs, they are typical cases in which practical applications of alloys benefit from the design of macroscopic chemical gradients, which can provide insights for the design of high-performance MPEAs.

6. Discussion and Conclusions

Multi-principal element alloys, especially medium-/high-entropy alloys, have received extensive attention from many researchers, mainly because of their compositional complexity, which leads to the greatly improved designability of such alloys. To better understand the relationship between their chemical structure and mechanical properties, research on chemical inhomogeneity should be expanded to other types of alloy, rather than concentrating on FCC alloys as is currently the case. Considering the complexity of the design and the tuning of chemical microstructure, computer simulation can certainly be beneficial in this respect. The most recent developments in experimental methods, such as heat treatment methods and microstructural observation methods, continue to promote the study of chemical inhomogeneity as well.

The formation of chemical inhomogeneities in MPEAs is highly dependent on the alloying constituents and the experimental treatment process. As proposed by Ding et al. [27], there is a distinct difference in chemical structure between CrMnFeCoNi and CrFeCoNiPd HEAs. Because the atomic size and electronegativity of Pd atoms are obviously different from those of other elements, the addition of the Pd element causes all elements to show a

stronger aggregation tendency. However, CrMnFeCoNi also shows a relatively random and uniform concentration distribution. The type, content and distribution of alloying elements have a considerable influence on the formation of the chemical structure. In addition, the degree of chemical inhomogeneity will be impacted by the experimental treatment method, including annealing time, temperature, etc. In line with the preceding discussion, this explains why many studies have come to rather disparate findings regarding the chemical inhomogeneity of alloys. Hence, not only should the composition and proportion be determined when investigating a particular chemical inhomogeneity, but the experimental processing technology should also be properly controlled. In this approach, it is possible to qualitatively or quantitatively explore the causes and effects of chemical inhomogeneity, while also guaranteeing the reproducibility of an experiment or computer simulation. The study of the chemical structure design in MPEAs is still in its early stages, and further research is still required to fully understand how the element types and compositional undulation of MPEAs affect the microscopic deformation process and macroscopic mechanical properties. There are even more high-performance alloys to be explored and discovered thanks to the variety of elements and experimental techniques. Future work can concentrate on exploring the microscopic mechanism of the effect of chemical structure design on mechanical characteristics and utilizing the relationship between chemical distribution and mechanical properties to obtain the optimal design of MPEAs.

The present article reviews chemical inhomogeneities from the atomic to the macroscale and their effects on the mechanical properties and deformation mechanisms of multi-principal element alloys. The main contents can be summarized as follows:

1. Due to the mismatch in atomic size and the complex electromagnetic interactions between different elements, the existence of LCO is inevitable, and the degree of LCO can be adjusted by manipulating the heating process or adding some substitute alloying elements, etc. In MPEAs with compositional inhomogeneity, especially in the case of naturally occurring CSRO during annealing, the increasing energy barrier for dislocation nucleation is beneficial for enhancing the yield strength of the alloys. Due to the differences in local strength and plasticity, areas with better performance are treated as obstacles, which will facilitate strengthening. This will reduce the speed of dislocation movement and promote dislocation cross-slip. At this time, the possibility of interaction between dislocations increases, which can promote the multiplication and pile-up of dislocations, resulting in an increase in the flow stress and strain hardening rate during plastic deformation.
2. Segregation causes varying degrees of chemical inhomogeneity at the nanoscale. The interaction between the segregated atoms and the dislocations affects the morphology and the slip velocity of the dislocations. In addition, grain boundary segregation can reduce grain boundary energy, improving the fracture toughness and the strength of the alloys, but it may lead to grain boundary embrittlement. Furthermore, stacking fault segregation may increase the creep strength of the alloys by slowing down the formation of twins. The segregation of different elements in the vicinity of various defects can have disparate effects on mechanical properties. Therefore, the effect of segregation on the dislocation behavior and mechanical properties needs to be analyzed depending on the specific conditions.
3. Experimentally, the ratio of the alloying elements can be controlled during the smelting process in order to synthesize alloys consisting of alternately laminated alloys with macroscopic compositional fluctuations. This will result in various scales of length and forms of compositional inhomogeneity in MPEAs with single-phase, dual-phase, and even multiphase structures. In fact, the inhomogeneous distribution of different elements is a prerequisite for the formation of dual-phase or multiphase structures. The compositional complexity of MPEAs is conducive to the adjustment of local SFE, promoting the occurrence of twinning, phase transition and defect storage, which can not only hinder dislocation movement, but can also improve the plastic deformation capacity of the alloys.

To date, a number of studies have investigated CSRO, nanoscale and larger-scale compositional fluctuations, probing their effects on the deformation mechanisms and mechanical properties. Although the results may be controversial, there is no doubt that the optimal design of compositional inhomogeneity can improve the overall performance of MPEAs. However, due to the difficulty of experimental preparation, most of these researches has been devoted to exploring different preparation techniques, while the research on microscopic deformation mechanisms and mechanical properties is very limited. Further efforts are required in this field concerning larger-scale compositional inhomogeneity in the future. It is noteworthy that the development of high-performance MPEAs may be achieved by cross-scale design of chemical inhomogeneity, such as controlling larger-scale element concentration fluctuations while tailoring CSRO, which is expected to be able to effectively enhance strength–plasticity synergy.

Author Contributions: Conceptualization, X.H., L.S. and J.Z.; data curation, L.S.; validation, D.L. and L.Z.; investigation, D.L. and J.Z.; writing—original draft preparation, J.Z.; writing—review and editing, L.Z. and L.S.; funding, X.H. and L.S. All authors have read and agreed to the published version of the manuscript.

Funding: This work is supported by the Research Grants Council of the Hong Kong Special Administrative Region, China under grant number CityU 11203022; the National Natural Science Foundation of China under grant number 12002108; the Guangdong Basic and Applied Basic Research Foundation under grant numbers 2020A1515110236 and 2022A1515011402; and the Shenzhen Municipal Science and Technology Innovation Council under grant number ZDSYS20210616110000001.

Data Availability Statement: No new data were created in this study. Data sharing is not applicable to this article.

Conflicts of Interest: The authors declare no conflict of interest.

References

1. Li, Z.; Pradeep, K.G.; Deng, Y.; Raabe, D.; Tasan, C.C. Metastable high-entropy dual-phase alloys overcome the strength–ductility trade-off. *Nature* **2016**, *534*, 227–230. [CrossRef] [PubMed]
2. Lei, Z.; Liu, X.; Wu, Y.; Wang, H.; Jiang, S.; Wang, S.; Hui, X.; Wu, Y.; Gault, B.; Kontis, P. Enhanced strength and ductility in a high-entropy alloy via ordered oxygen complexes. *Nature* **2018**, *563*, 546–550. [CrossRef] [PubMed]
3. Li, W.; Liaw, P.K.; Gao, Y. Fracture resistance of high entropy alloys: A review. *Intermetallics* **2018**, *99*, 69–83. [CrossRef]
4. Wu, Z.; Bei, H.; Pharr, G.M.; George, E.P. Temperature dependence of the mechanical properties of equiatomic solid solution alloys with face-centered cubic crystal structures. *Acta Mater.* **2014**, *81*, 428–441. [CrossRef]
5. Gavriljuk, V.; Shanina, B.; Berns, H. Ab initio development of a high-strength corrosion-resistant austenitic steel. *Acta Mater.* **2008**, *56*, 5071–5082. [CrossRef]
6. Ayyagari, A.; Hasannaeimi, V.; Grewal, H.S.; Arora, H.; Mukherjee, S. Corrosion, erosion and wear behavior of complex concentrated alloys: A review. *Metals* **2018**, *8*, 603. [CrossRef]
7. Chuang, M.-H.; Tsai, M.-H.; Wang, W.-R.; Lin, S.-J.; Yeh, J.-W. Microstructure and wear behavior of $Al_xCo_{1.5}CrFeNi_{1.5}Ti_y$ high-entropy alloys. *Acta Mater.* **2011**, *59*, 6308–6317. [CrossRef]
8. Jiang, Z.; He, J.; Wang, H.; Zhang, H.; Lu, Z.; Dai, L. Shock compression response of high entropy alloys. *Mater. Res. Lett.* **2016**, *4*, 226–232. [CrossRef]
9. Zhang, T.; Ma, S.; Zhao, D.; Wu, Y.; Zhang, Y.; Wang, Z.; Qiao, J. Simultaneous enhancement of strength and ductility in a NiCoCrFe high-entropy alloy upon dynamic tension: Micromechanism and constitutive modeling. *Int. J. Plast.* **2020**, *124*, 226–246. [CrossRef]
10. Zhang, Y.; Liu, M.; Sun, J.; Li, G.; Zheng, R.; Xiao, W.; Ma, C. Excellent thermal stability and mechanical properties of bulk nanostructured FeCoNiCu high entropy alloy. *Mater. Sci. Eng. A* **2022**, *835*, 142670. [CrossRef]
11. Chen, J.; Zhou, X.; Wang, W.; Liu, B.; Lv, Y.; Yang, W.; Xu, D.; Liu, Y. A review on fundamental of high entropy alloys with promising high–temperature properties. *J. Alloy. Compd.* **2018**, *760*, 15–30. [CrossRef]
12. Sun, L.G.; Wu, G.; Wang, Q.; Lu, J. Nanostructural metallic materials: Structures and mechanical properties. *Mater. Today* **2020**, *38*, 114–135. [CrossRef]
13. Li, X.; Wei, Y.; Lu, L.; Lu, K.; Gao, H. Dislocation nucleation governed softening and maximum strength in nano-twinned metals. *Nature* **2010**, *464*, 877–880. [CrossRef] [PubMed]
14. Sun, L.; He, X.; Lu, J. Nanotwinned and hierarchical nanotwinned metals: A review of experimental, computational and theoretical efforts. *Npj Comput. Mater.* **2018**, *4*, 6. [CrossRef]

15. Chen, A.; Zhu, L.; Sun, L.; Liu, J.; Wang, H.; Wang, X.; Yang, J.; Lu, J. Scale law of complex deformation transitions of nanotwins in stainless steel. *Nat. Commun.* **2019**, *10*, 1403. [CrossRef]
16. Sun, L.; Li, D.; Zhu, L.; Ruan, H.; Lu, J. Size-dependent formation and thermal stability of high-order twins in hierarchical nanotwinned metals. *Int. J. Plast.* **2020**, *128*, 102685. [CrossRef]
17. Lu, K.; Lu, L.; Suresh, S. Strengthening Materials by Engineering Coherent Internal Boundaries at the Nanoscale. *Science* **2009**, *324*, 349–352. [CrossRef]
18. Sun, L.G.; He, X.Q.; Zhu, L.L.; Lu, J. Two softening stages in nanotwinned Cu. *Philos. Mag.* **2014**, *94*, 4037–4052. [CrossRef]
19. Sun, L.; He, X.; Lu, J. Understanding the mechanical characteristics of nanotwinned diamond by atomistic simulations. *Carbon* **2018**, *127*, 320–328. [CrossRef]
20. Liu, X.; Sun, L.; Zhu, L.; Liu, J.; Lu, K.; Lu, J. High-order hierarchical nanotwins with superior strength and ductility. *Acta Mater.* **2018**, *149*, 397–406. [CrossRef]
21. Jang, D.; Li, X.; Gao, H.; Greer, J.R. Deformation mechanisms in nanotwinned metal nanopillars. *Nat. Nanotechnol.* **2012**, *7*, 594–601. [CrossRef] [PubMed]
22. You, Z.; Li, X.; Gui, L.; Lu, Q.; Zhu, T.; Gao, H.; Lu, L. Plastic anisotropy and associated deformation mechanisms in nanotwinned metals. *Acta Mater.* **2013**, *61*, 217–227. [CrossRef]
23. Sun, L.; He, X.; Wang, J.; Lu, J. Deformation and failure mechanisms of nanotwinned copper films with a pre-existing crack. *Mater. Sci. Eng. A* **2014**, *606*, 334–345. [CrossRef]
24. Sun, L.; He, X.; Lu, J. Atomistic simulation study on twin orientation and spacing distribution effects on nanotwinned Cu films. *Philos. Mag.* **2015**, *95*, 3467–3485. [CrossRef]
25. Zhang, F.; Zhao, S.; Jin, K.; Xue, H.; Velisa, G.; Bei, H.; Huang, R.; Ko, J.; Pagan, D.; Neuefeind, J. Local structure and short-range order in a NiCoCr solid solution alloy. *Phys. Rev. Lett.* **2017**, *118*, 205501. [CrossRef] [PubMed]
26. Zhang, R.; Zhao, S.; Ding, J.; Chong, Y.; Jia, T.; Ophus, C.; Asta, M.; Ritchie, R.O.; Minor, A.M. Short-range order and its impact on the CrCoNi medium-entropy alloy. *Nature* **2020**, *581*, 283–287. [CrossRef]
27. Ding, Q.; Zhang, Y.; Chen, X.; Fu, X.; Chen, D.; Chen, S.; Gu, L.; Wei, F.; Bei, H.; Gao, Y.; et al. Tuning element distribution, structure and properties by composition in high-entropy alloys. *Nature* **2019**, *574*, 223–227. [CrossRef]
28. Widom, M.; Huhn, W.P.; Maiti, S.; Steurer, W. Hybrid Monte Carlo/molecular dynamics simulation of a refractory metal high entropy alloy. *Metall. Mater. Trans. A* **2014**, *45*, 196–200. [CrossRef]
29. Tamm, A.; Aabloo, A.; Klintenberg, M.; Stocks, M.; Caro, A. Atomic-scale properties of Ni-based FCC ternary, and quaternary alloys. *Acta Mater.* **2015**, *99*, 307–312. [CrossRef]
30. Ma, Y.; Wang, Q.; Li, C.; Santodonato, L.J.; Feygenson, M.; Dong, C.; Liaw, P.K. Chemical short-range orders and the induced structural transition in high-entropy alloys. *Scr. Mater.* **2018**, *144*, 64–68. [CrossRef]
31. Ding, J.; Yu, Q.; Asta, M.; Ritchie, R.O. Tunable stacking fault energies by tailoring local chemical order in CrCoNi medium-entropy alloys. *Proc. Natl. Acad. Sci. USA* **2018**, *115*, 8919–8924. [CrossRef] [PubMed]
32. Li, Q.-J.; Sheng, H.; Ma, E. Strengthening in multi-principal element alloys with local-chemical-order roughened dislocation pathways. *Nat. Commun.* **2019**, *10*, 3563. [CrossRef] [PubMed]
33. Yuan, L.; Tao, R.; Wen, P.; Li, J.; Wang, S.; Li, D. Molecular dynamics simulation of chemical short-range order strengthening in FCC FeNiCrCoAlx alloys. *Phys. B Condens. Matter* **2023**, *649*, 414447. [CrossRef]
34. Tang, G.; Zhang, Z.; Liu, Y.; Wang, Y.; Wu, X.; Liu, X. Quantifying chemical fluctuations around medium-range orders and its impact on dislocation interactions in equiatomic CrCoNi medium entropy alloy. *Mater. Des.* **2023**, *225*, 111572. [CrossRef]
35. Singh, P.; Smirnov, A.V.; Johnson, D.D. Atomic short-range order and incipient long-range order in high-entropy alloys. *Phys. Rev. B* **2015**, *91*, 224204. [CrossRef]
36. Jian, W.-R.; Xie, Z.; Xu, S.; Su, Y.; Yao, X.; Beyerlein, I.J. Effects of lattice distortion and chemical short-range order on the mechanisms of deformation in medium entropy alloy CoCrNi. *Acta Mater.* **2020**, *199*, 352–369. [CrossRef]
37. Oh, H.S.; Kim, S.J.; Odbadrakh, K.; Ryu, W.H.; Yoon, K.N.; Mu, S.; Körmann, F.; Ikeda, Y.; Tasan, C.C.; Raabe, D. Engineering atomic-level complexity in high-entropy and complex concentrated alloys. *Nat. Commun.* **2019**, *10*, 2090. [CrossRef]
38. Fernández-Caballero, A.; Wróbel, J.S.; Mummery, P.M.; Nguyen-Manh, D. Short-Range Order in High Entropy Alloys: Theoretical Formulation and Application to Mo-Nb-Ta-V-W System. *J. Phase Equilibria Diffus.* **2017**, *38*, 391–403. [CrossRef]
39. Li, Y.; Savan, A.; Kostka, A.; Stein, H.; Ludwig, A. Accelerated atomic-scale exploration of phase evolution in compositionally complex materials. *Mater. Horiz.* **2018**, *5*, 86–92. [CrossRef]
40. Li, L.; Chen, Z.; Kuroiwa, S.; Ito, M.; Yuge, K.; Kishida, K.; Tanimoto, H.; Yu, Y.; Inui, H.; George, E.P. Evolution of short-range order and its effects on the plastic deformation behavior of single crystals of the equiatomic Cr-Co-Ni medium-entropy alloy. *Acta Mater.* **2023**, *243*, 118537. [CrossRef]
41. Li, Z.; Raabe, D. Influence of compositional inhomogeneity on mechanical behavior of an interstitial dual-phase high-entropy alloy. *Mater. Chem. Phys.* **2018**, *210*, 29–36. [CrossRef]
42. Xun, K.; Zhang, B.; Wang, Q.; Zhang, Z.; Ding, J.; Ma, E. Local chemical inhomogeneities in TiZrNb-based refractory high-entropy alloys. *J. Mater. Sci. Technol.* **2023**, *135*, 221–230. [CrossRef]
43. Chen, X.; Wang, Q.; Cheng, Z.; Zhu, M.; Zhou, H.; Jiang, P.; Zhou, L.; Xue, Q.; Yuan, F.; Zhu, J. Direct observation of chemical short-range order in a medium-entropy alloy. *Nature* **2021**, *592*, 712–716. [CrossRef] [PubMed]

44. Zhou, L.; Wang, Q.; Wang, J.; Chen, X.; Jiang, P.; Zhou, H.; Yuan, F.; Wu, X.; Cheng, Z.; Ma, E. Atomic-scale evidence of chemical short-range order in CrCoNi medium-entropy alloy. *Acta Mater.* **2022**, *224*, 117490. [CrossRef]
45. Cao, F.-H.; Wang, Y.-J.; Dai, L.-H. Novel atomic-scale mechanism of incipient plasticity in a chemically complex CrCoNi medium-entropy alloy associated with inhomogeneity in local chemical environment. *Acta Mater.* **2020**, *194*, 283–294. [CrossRef]
46. Bu, Y.; Wu, Y.; Lei, Z.; Yuan, X.; Wu, H.; Feng, X.; Liu, J.; Ding, J.; Lu, Y.; Wang, H.; et al. Local chemical fluctuation mediated ductility in body-centered-cubic high-entropy alloys. *Mater. Today* **2021**, *46*, 28–34. [CrossRef]
47. Smith, T.M.; Esser, B.D.; Good, B.; Hooshmand, M.S.; Viswanathan, G.B.; Rae, C.M.F.; Ghazisaeidi, M.; McComb, D.W.; Mills, M.J. Segregation and Phase Transformations Along Superlattice Intrinsic Stacking Faults in Ni-Based Superalloys. *Metall. Mater. Trans. A* **2018**, *49*, 4186–4198. [CrossRef]
48. Jensen, J.; Welk, B.; Williams, R.; Sosa, J.; Huber, D.; Senkov, O.; Viswanathan, G.; Fraser, H. Characterization of the microstructure of the compositionally complex alloy $Al_1Mo_{0.5}Nb_1Ta_{0.5}Ti_1Zr_1$. *Scr. Mater.* **2016**, *121*, 1–4. [CrossRef]
49. Chang, R.; Fang, W.; Yu, H.; Bai, X.; Zhang, X.; Liu, B.; Yin, F. Heterogeneous banded precipitation of $(CoCrNi)_{93}Mo_7$ medium entropy alloys towards strength–ductility synergy utilizing compositional inhomogeneity. *Scr. Mater.* **2019**, *172*, 144–148. [CrossRef]
50. Kuczyk, M.; Kotte, L.; Kaspar, J.; Zimmermann, M.; Leyens, C. Alloy Design and Microstructure Evolution in the AlxCoCrFeNi Alloy System Synthesized by Laser Metal Deposition. *Front. Mater.* **2020**, *7*, 242. [CrossRef]
51. Fatermans, J.; Van Aert, S.; den Dekker, A.-J. The maximum a posteriori probability rule for atom column detection from HAADF STEM images. *Ultramicroscopy* **2019**, *201*, 81–91. [CrossRef] [PubMed]
52. Wu, Y.; Zhang, F.; Yuan, X.; Huang, H.; Wen, X.; Wang, Y.; Zhang, M.; Wu, H.; Liu, X.; Wang, H.; et al. Short-range ordering and its effects on mechanical properties of high-entropy alloys. *J. Mater. Sci. Technol.* **2021**, *62*, 214–220. [CrossRef]
53. Ceguerra, A.V.; Moody, M.P.; Powles, R.C.; Petersen, T.C.; Marceau, R.K.; Ringer, S.P. Short-range order in multicomponent materials. *Acta Crystallogr. Sect. A Found. Crystallogr.* **2012**, *68*, 547–560. [CrossRef] [PubMed]
54. Hu, R.; Jin, S.; Sha, G. Application of atom probe tomography in understanding high entropy alloys: 3D local chemical compositions in atomic scale analysis. *Prog. Mater Sci.* **2022**, *123*, 100854. [CrossRef]
55. Koch, L.; Granberg, F.; Brink, T.; Utt, D.; Albe, K.; Djurabekova, F.; Nordlund, K. Local segregation versus irradiation effects in high-entropy alloys: Steady-state conditions in a driven system. *J. Appl. Phys.* **2017**, *122*, 105106. [CrossRef]
56. Ji, W.; Wu, M.S. Inhibiting the inverse Hall-Petch behavior in CoCuFeNiPd high-entropy alloys with short-range ordering and grain boundary segregation. *Scr. Mater.* **2022**, *221*, 114950. [CrossRef]
57. Salloom, R.; Baskes, M.I.; Srinivasan, S.G. Atomic level simulations of the phase stability and stacking fault energy of FeCoCrMnSi high entropy alloy. *Modell. Simul. Mater. Sci. Eng.* **2022**, *30*, 075002. [CrossRef]
58. Feng, R.; Liaw, P.K.; Gao, M.C.; Widom, M. First-principles prediction of high-entropy-alloy stability. *Npj Comput. Mater.* **2017**, *3*, 50. [CrossRef]
59. Huang, S.; Li, W.; Lu, S.; Tian, F.; Shen, J.; Holmström, E.; Vitos, L. Temperature dependent stacking fault energy of FeCrCoNiMn high entropy alloy. *Scr. Mater.* **2015**, *108*, 44–47. [CrossRef]
60. Ericsson, T. The temperature and concentration dependence of the stacking fault energy in the Co-Ni system. *Acta Metall.* **1966**, *14*, 853–865. [CrossRef]
61. Ikeda, Y.; Körmann, F.; Tanaka, I.; Neugebauer, J. Impact of chemical fluctuations on stacking fault energies of CrCoNi and CrMnFeCoNi high entropy alloys from first principles. *Entropy* **2018**, *20*, 655. [CrossRef] [PubMed]
62. Deng, Y.; Tasan, C.C.; Pradeep, K.G.; Springer, H.; Kostka, A.; Raabe, D. Design of a twinning-induced plasticity high entropy alloy. *Acta Mater.* **2015**, *94*, 124–133. [CrossRef]
63. Wei, D.; Li, X.; Heng, W.; Koizumi, Y.; He, F.; Choi, W.-M.; Lee, B.-J.; Kim, H.S.; Kato, H.; Chiba, A. Novel Co-rich high entropy alloys with superior tensile properties. *Mater. Res. Lett.* **2019**, *7*, 82–88. [CrossRef]
64. Wei, D.; Li, X.; Jiang, J.; Heng, W.; Koizumi, Y.; Choi, W.-M.; Lee, B.-J.; Kim, H.S.; Kato, H.; Chiba, A. Novel Co-rich high performance twinning-induced plasticity (TWIP) and transformation-induced plasticity (TRIP) high-entropy alloys. *Scr. Mater.* **2019**, *165*, 39–43. [CrossRef]
65. Xie, Z.; Jian, W.-R.; Xu, S.; Beyerlein, I.J.; Zhang, X.; Yao, X.; Zhang, R. Phase transition in medium entropy alloy CoCrNi under quasi-isentropic compression. *Int. J. Plast.* **2022**, *157*, 103389. [CrossRef]
66. Miao, J.; Slone, C.; Smith, T.; Niu, C.; Bei, H.; Ghazisaeidi, M.; Pharr, G.; Mills, M.J. The evolution of the deformation substructure in a Ni-Co-Cr equiatomic solid solution alloy. *Acta Mater.* **2017**, *132*, 35–48. [CrossRef]
67. Sun, P.-L.; Zhao, Y.; Cooley, J.; Kassner, M.; Horita, Z.; Langdon, T.; Lavernia, E.; Zhu, Y. Effect of stacking fault energy on strength and ductility of nanostructured alloys: An evaluation with minimum solution hardening. *Mater. Sci. Eng. A* **2009**, *525*, 83–86. [CrossRef]
68. Bahmanpour, H.; Kauffmann, A.; Khoshkhoo, M.; Youssef, K.; Mula, S.; Freudenberger, J.; Eckert, J.; Scattergood, R.; Koch, C. Effect of stacking fault energy on deformation behavior of cryo-rolled copper and copper alloys. *Mater. Sci. Eng. A* **2011**, *529*, 230–236. [CrossRef]
69. Youssef, K.; Sakaliyska, M.; Bahmanpour, H.; Scattergood, R.; Koch, C. Effect of stacking fault energy on mechanical behavior of bulk nanocrystalline Cu and Cu alloys. *Acta Mater.* **2011**, *59*, 5758–5764. [CrossRef]
70. Gong, Y.; Wen, C.; Li, Y.; Wu, X.; Cheng, L.; Han, X.; Zhu, X. Simultaneously enhanced strength and ductility of Cu–xGe alloys through manipulating the stacking fault energy (SFE). *Mater. Sci. Eng. A* **2013**, *569*, 144–149. [CrossRef]

71. Eleti, R.R.; Stepanov, N.; Yurchenko, N.; Klimenko, D.; Zherebtsov, S. Plastic deformation of solid-solution strengthened Hf-Nb-Ta-Ti-Zr body-centered cubic medium/high-entropy alloys. *Scr. Mater.* **2021**, *200*, 113927. [CrossRef]
72. LaRosa, C.R.; Shih, M.; Varvenne, C.; Ghazisaeidi, M. Solid solution strengthening theories of high-entropy alloys. *Mater. Charact.* **2019**, *151*, 310–317. [CrossRef]
73. Yang, X.; Xi, Y.; He, C.; Chen, H.; Zhang, X.; Tu, S. Chemical short-range order strengthening mechanism in CoCrNi medium-entropy alloy under nanoindentation. *Scr. Mater.* **2022**, *209*, 114364. [CrossRef]
74. Ma, S.; Zhang, J.; Xu, B.; Xiong, Y.; Shao, W.; Zhao, S. Chemical short-range ordering regulated dislocation cross slip in high-entropy alloys. *J. Alloy. Compd.* **2022**, *911*, 165144. [CrossRef]
75. Zhao, Y.K.; Park, J.M.; Jang, J.I.; Ramamurty, U. Bimodality of incipient plastic strength in face-centered cubic high-entropy alloys. *Acta Mater.* **2021**, *202*, 124–134. [CrossRef]
76. Antillon, E.; Woodward, C.; Rao, S.I.; Akdim, B.; Parthasarathy, T.A. Chemical short range order strengthening in a model FCC high entropy alloy. *Acta Mater.* **2020**, *190*, 29–42. [CrossRef]
77. Ma, E. Unusual dislocation behavior in high-entropy alloys. *Scr. Mater.* **2020**, *181*, 127–133. [CrossRef]
78. Niu, C.; LaRosa, C.R.; Miao, J.; Mills, M.J.; Ghazisaeidi, M. Magnetically-driven phase transformation strengthening in high entropy alloys. *Nat. Commun.* **2018**, *9*, 1363. [CrossRef]
79. Zeng, Y.; Cai, X.; Koslowski, M. Effects of the stacking fault energy fluctuations on the strengthening of alloys. *Acta Mater.* **2019**, *164*, 1–11. [CrossRef]
80. Zhang, L.; Xiang, Y.; Han, J.; Srolovitz, D.J. The effect of randomness on the strength of high-entropy alloys. *Acta Mater.* **2019**, *166*, 424–434. [CrossRef]
81. Utt, D.; Lee, S.; Xing, Y.; Jeong, H.; Stukowski, A.; Oh, S.H.; Dehm, G.; Albe, K. The origin of jerky dislocation motion in high-entropy alloys. *Nat. Commun.* **2022**, *13*, 4777. [CrossRef] [PubMed]
82. Moon, J.; Bouaziz, O.; Kim, H.S.; Estrin, Y. Twinning engineering of a CoCrFeMnNi high-entropy alloy. *Scr. Mater.* **2021**, *197*, 113808. [CrossRef]
83. Sun, Z.; Shi, C.; Liu, C.; Shi, H.; Zhou, J. The effect of short-range order on mechanical properties of high entropy alloy $Al_{0.3}$CoCrFeNi. *Mater. Des.* **2022**, *223*, 111214. [CrossRef]
84. He, M.; Shen, Y.; Jia, N.; Liaw, P. C and N doping in high-entropy alloys: A pathway to achieve desired strength-ductility synergy. *Appl. Mater. Today* **2021**, *25*, 101162. [CrossRef]
85. Püschl, W. Models for dislocation cross-slip in close-packed crystal structures: A critical review. *Prog. Mater Sci.* **2002**, *47*, 415–461. [CrossRef]
86. Yin, B.; Yoshida, S.; Tsuji, N.; Curtin, W.A. Yield strength and misfit volumes of NiCoCr and implications for short-range-order. *Nat. Commun.* **2020**, *11*, 2507. [CrossRef]
87. Ding, Q.; Li, S.; Chen, L.-Q.; Han, X.; Zhang, Z.; Yu, Q.; Li, J. Re segregation at interfacial dislocation network in a nickel-based superalloy. *Acta Mater.* **2018**, *154*, 137–146. [CrossRef]
88. Hu, S.; Chen, L. Solute segregation and coherent nucleation and growth near a dislocation—A phase-field model integrating defect and phase microstructures. *Acta Mater.* **2001**, *49*, 463–472. [CrossRef]
89. Kang, Y.B.; Shim, S.H.; Lee, K.H.; Hong, S.I. Dislocation creep behavior of CoCrFeMnNi high entropy alloy at intermediate temperatures. *Mater. Res. Lett.* **2018**, *6*, 689–695. [CrossRef]
90. Raabe, D.; Herbig, M.; Sandlöbes, S.; Li, Y.; Tytko, D.; Kuzmina, M.; Ponge, D.; Choi, P.-P. Grain boundary segregation engineering in metallic alloys: A pathway to the design of interfaces. *Curr. Opin. Solid State Mater. Sci.* **2014**, *18*, 253–261. [CrossRef]
91. Liu, F.; Kirchheim, R. Grain boundary saturation and grain growth. *Scr. Mater.* **2004**, *51*, 521–525. [CrossRef]
92. Lejček, P.; Hofmann, S. Thermodynamics and structural aspects of grain boundary segregation. *Crit. Rev. Solid State Mater. Sci.* **1995**, *20*, 1–85. [CrossRef]
93. Raabe, D.; Sandlöbes, S.; Millán, J.; Ponge, D.; Assadi, H.; Herbig, M.; Choi, P.-P. Segregation engineering enables nanoscale martensite to austenite phase transformation at grain boundaries: A pathway to ductile martensite. *Acta Mater.* **2013**, *61*, 6132–6152. [CrossRef]
94. Sangid, M.D.; Sehitoglu, H.; Maier, H.J.; Niendorf, T. Grain boundary characterization and energetics of superalloys. *Mater. Sci. Eng. A* **2010**, *527*, 7115–7125. [CrossRef]
95. Pradeep, K.; Wanderka, N.; Choi, P.; Banhart, J.; Murty, B.; Raabe, D. Atomic-scale compositional characterization of a nanocrystalline AlCrCuFeNiZn high-entropy alloy using atom probe tomography. *Acta Mater.* **2013**, *61*, 4696–4706. [CrossRef]
96. Buban, J.P.; Mizoguchi, T.; Shibata, N.; Abe, E.; Yamamoto, T.; Ikuhara, Y. Zr segregation and associated Al vacancies in alumina grain boundaries. *J. Ceram. Soc. Jpn.* **2011**, *119*, 840–844. [CrossRef]
97. Detor, A.J.; Schuh, C.A. Grain boundary segregation, chemical ordering and stability of nanocrystalline alloys: Atomistic computer simulations in the Ni–W system. *Acta Mater.* **2007**, *55*, 4221–4232. [CrossRef]
98. Pan, Z.; Sansoz, F. Heterogeneous solute segregation suppresses strain localization in nanocrystalline Ag-Ni alloys. *Acta Mater.* **2020**, *200*, 91–100. [CrossRef]
99. Picard, E.-A.; Sansoz, F. Ni solute segregation and associated plastic deformation mechanisms into random FCC Ag, BCC Nb and HCP Zr polycrystals. *Acta Mater.* **2022**, *240*, 118367. [CrossRef]
100. Sansoz, F.; Ke, X. Hall–Petch strengthening limit through partially active segregation in nanocrystalline Ag-Cu alloys. *Acta Mater.* **2022**, *225*, 117560. [CrossRef]

101. McCarthy, M.J.; Zheng, H.; Apelian, D.; Bowman, W.J.; Hahn, H.; Luo, J.; Ong, S.P.; Pan, X.; Rupert, T.J. Emergence of near-boundary segregation zones in face-centered cubic multiprincipal element alloys. *Phys. Rev. Mater.* **2021**, *5*, 113601. [CrossRef]
102. Hong, S.I. Influence of dynamic strain aging on the dislocation substructure in a uniaxial tension test. *Mater. Sci. Eng.* **1986**, *79*, 1–7. [CrossRef]
103. Hong, S.I. Criteria for predicting twin-induced plasticity in solid solution copper alloys. *Mater. Sci. Eng. A* **2018**, *711*, 492–497. [CrossRef]
104. Chaudhury, P.K.; Mohamed, F.A. Creep characteristics of an Al 2 wt.% Cu alloy in the solid solution range. *Mater. Sci. Eng. A* **1988**, *101*, 13–23.
105. King, H. Quantitative size-factors for metallic solid solutions. *J. Mater. Sci.* **1966**, *1*, 79–90. [CrossRef]
106. Farid, Z.; Mahmoud, S.; Ali, A.; El-Naquib, N. On the Transition in Creep Behaviour during Primary Creep of Cu-Zn Alloys. *Phys. Status Solidi A* **1990**, *117*, 437–446. [CrossRef]
107. Hong, S.-H.; Weertman, J. High temperature creep of ordered and disordered beta brass—II. Internal stress. *Acta Metall.* **1986**, *34*, 743–751. [CrossRef]
108. Hong, S.I.; Laird, C. Mechanisms of slip mode modification in FCC solid solutions. *Acta Metall. Mater.* **1990**, *38*, 1581–1594. [CrossRef]
109. Wynblatt, P.; Chatain, D. Modeling grain boundary and surface segregation in multicomponent high-entropy alloys. *Phys. Rev. Mater.* **2019**, *3*, 054004. [CrossRef]
110. Li, L.; Li, Z.; da Silva, A.K.; Peng, Z.; Zhao, H.; Gault, B.; Raabe, D. Segregation-driven grain boundary spinodal decomposition as a pathway for phase nucleation in a high-entropy alloy. *Acta Mater.* **2019**, *178*, 1–9. [CrossRef]
111. Li, L.; Kamachali, R.D.; Li, Z.; Zhang, Z. Grain boundary energy effect on grain boundary segregation in an equiatomic high-entropy alloy. *Phys. Rev. Mater.* **2020**, *4*, 053603. [CrossRef]
112. Ferrari, A.; Körmann, F. Surface segregation in Cr-Mn-Fe-Co-Ni high entropy alloys. *Appl. Surf. Sci.* **2020**, *533*, 147471. [CrossRef]
113. Kapoor, M.; Kaub, T.; Darling, K.A.; Boyce, B.L.; Thompson, G.B. An atom probe study on Nb solute partitioning and nanocrystalline grain stabilization in mechanically alloyed Cu-Nb. *Acta Mater.* **2017**, *126*, 564–575. [CrossRef]
114. Zhang, F.; Li, G.; Zhu, D.; Zhou, J. Grain size effect on the mechanical behaviors in nanocrystalline Cu-Ag alloy with grain boundary affect zone segregation. *Mater. Lett.* **2020**, *278*, 128406. [CrossRef]
115. Li, G.; Wang, R.; Zhang, F.; Zhu, D.; Li, F.; Zhou, J. Titanium content and columnar particles effect on the deformation behaviors of nanocrystalline Ni–Ti alloy with GBAZ segregation. *Appl. Phys. A* **2023**, *129*, 152. [CrossRef]
116. Weissmüller, J. Alloy effects in nanostructures. *Nanostruct. Mater.* **1993**, *3*, 261–272. [CrossRef]
117. Kirchheim, R. Grain coarsening inhibited by solute segregation. *Acta Mater.* **2002**, *50*, 413–419. [CrossRef]
118. Chookajorn, T.; Murdoch, H.A.; Schuh, C.A. Design of stable nanocrystalline alloys. *Science* **2012**, *337*, 951–954. [CrossRef]
119. Millett, P.C.; Selvam, R.P.; Saxena, A. Improving grain boundary sliding resistance with segregated dopants. *Mater. Sci. Eng. A* **2006**, *431*, 92–99. [CrossRef]
120. Vo, N.Q.; Averback, R.S.; Bellon, P.; Caro, A. Yield strength in nanocrystalline Cu during high strain rate deformation. *Scr. Mater.* **2009**, *61*, 76–79. [CrossRef]
121. Vo, N.; Schäfer, J.; Averback, R.; Albe, K.; Ashkenazy, Y.; Bellon, P. Reaching theoretical strengths in nanocrystalline Cu by grain boundary doping. *Scr. Mater.* **2011**, *65*, 660–663. [CrossRef]
122. Laporte, V.; Mortensen, A. Intermediate temperature embrittlement of copper alloys. *Int. Mater. Rev.* **2009**, *54*, 94–116. [CrossRef]
123. Zheng, L.; Schmitz, G.; Meng, Y.; Chellali, R.; Schlesiger, R. Mechanism of intermediate temperature embrittlement of Ni and Ni-based superalloys. *Crit. Rev. Solid State Mater. Sci.* **2012**, *37*, 181–214. [CrossRef]
124. Xu, T.; Zheng, L.; Wang, K.; Misra, R. Unified mechanism of intergranular embrittlement based on non-equilibrium grain boundary segregation. *Int. Mater. Rev.* **2013**, *58*, 263–295. [CrossRef]
125. Feng, L.; Rao, Y.; Ghazisaeidi, M.; Mills, M.J.; Wang, Y. Quantitative prediction of Suzuki segregation at stacking faults of the γ′ phase in Ni-base superalloys. *Acta Mater.* **2020**, *200*, 223–235. [CrossRef]
126. Rao, Y.; Smith, T.M.; Mills, M.J.; Ghazisaeidi, M. Segregation of alloying elements to planar faults in γ′-Ni3Al. *Acta Mater.* **2018**, *148*, 173–184. [CrossRef]
127. Smith, T.M.; Esser, B.D.; Antolin, N.; Viswanathan, G.B.; Hanlon, T.; Wessman, A.; Mourer, D.; Windl, W.; McComb, D.W.; Mills, M.J. Segregation and η phase formation along stacking faults during creep at intermediate temperatures in a Ni-based superalloy. *Acta Mater.* **2015**, *100*, 19–31. [CrossRef]
128. Smith, T.M.; Good, B.S.; Gabb, T.P.; Esser, B.D.; Egan, A.J.; Evans, L.J.; McComb, D.W.; Mills, M.J. Effect of stacking fault segregation and local phase transformations on creep strength in Ni-base superalloys. *Acta Mater.* **2019**, *172*, 55–65. [CrossRef]
129. Barba, D.; Smith, T.M.; Miao, J.; Mills, M.J.; Reed, R.C. Segregation-Assisted Plasticity in Ni-Based Superalloys. *Metall. Mater. Trans. A* **2018**, *49*, 4173–4185. [CrossRef]
130. Ming, K.; Bi, X.; Wang, J. Segregation of Mo atoms into stacking faults in CrFeCoNiMo alloy. *Philos. Mag.* **2019**, *99*, 1014–1024. [CrossRef]
131. Suzuki, H. Segregation of solute atoms to stacking faults. *J. Phys. Soc. Jpn.* **1962**, *17*, 322–325. [CrossRef]
132. Hirsch, P. A new theory of the anomalous yield stress in L12 alloys. *Philos. Mag. A* **1992**, *65*, 569–612. [CrossRef]
133. Paidar, V.; Pope, D.; Vitek, V. A theory of the anomalous yield behavior in L12 ordered alloys. *Acta Metall.* **1984**, *32*, 435–448. [CrossRef]

134. Zhu, Z.; Basoalto, H.; Warnken, N.; Reed, R. A model for the creep deformation behaviour of nickel-based single crystal superalloys. *Acta Mater.* **2012**, *60*, 4888–4900. [CrossRef]
135. Gao, S.; Fivel, M.; Ma, A.; Hartmaier, A. Influence of misfit stresses on dislocation glide in single crystal superalloys: A three-dimensional discrete dislocation dynamics study. *J. Mech. Phys. Solids* **2015**, *76*, 276–290. [CrossRef]
136. Gao, S.; Fivel, M.; Ma, A.; Hartmaier, A. 3D discrete dislocation dynamics study of creep behavior in Ni-base single crystal superalloys by a combined dislocation climb and vacancy diffusion model. *J. Mech. Phys. Solids* **2017**, *102*, 209–223. [CrossRef]
137. Huang, S.; Huang, M.; Li, Z. Effect of interfacial dislocation networks on the evolution of matrix dislocations in nickel-based superalloy. *Int. J. Plast.* **2018**, *110*, 1–18. [CrossRef]
138. Carroll, L.J.; Feng, Q.; Pollock, T. Interfacial dislocation networks and creep in directional coarsened Ru-containing nickel-base single-crystal superalloys. *Metall. Mater. Trans. A* **2008**, *39*, 1290–1307. [CrossRef]
139. Xiong, J.; Zhu, Y.; Li, Z.; Huang, M. Quantitative study on interactions between interfacial misfit dislocation networks and matrix dislocations in Ni-based single crystal superalloys. *Acta Mech. Solida Sin.* **2017**, *30*, 345–353. [CrossRef]
140. Li, Y.-L.; Wu, W.-P.; Ruan, Z.-G. Molecular dynamics simulation of the evolution of interfacial dislocation network and stress distribution of a Ni-based single-crystal superalloy. *Acta Metall. Sin.* **2016**, *29*, 689–696. [CrossRef]
141. Jacome, L.A.; Nörtershäuser, P.; Somsen, C.; Dlouhý, A.; Eggeler, G. On the nature of γ' phase cutting and its effect on high temperature and low stress creep anisotropy of Ni-base single crystal superalloys. *Acta Mater.* **2014**, *69*, 246–264. [CrossRef]
142. Hussein, A.M.; Rao, S.I.; Uchic, M.D.; Parthasarathy, T.A.; El-Awady, J.A. The strength and dislocation microstructure evolution in superalloy microcrystals. *J. Mech. Phys. Solids* **2017**, *99*, 146–162. [CrossRef]
143. Yang, H.; Li, Z.; Huang, M. Modeling dislocation cutting the precipitate in nickel-based single crystal superalloy via the discrete dislocation dynamics with SISF dissociation scheme. *Comput. Mater. Sci.* **2013**, *75*, 52–59. [CrossRef]
144. Yashiro, K.; Kurose, F.; Nakashima, Y.; Kubo, K.; Tomita, Y.; Zbib, H. Discrete dislocation dynamics simulation of cutting of γ' precipitate and interfacial dislocation network in Ni-based superalloys. *Int. J. Plast.* **2006**, *22*, 713–723. [CrossRef]
145. Smith, T.M.; Hooshmand, M.S.; Esser, B.D.; Otto, F.; McComb, D.W.; George, E.P.; Ghazisaeidi, M.; Mills, M.J. Atomic-scale characterization and modeling of 60 dislocations in a high-entropy alloy. *Acta Mater.* **2016**, *110*, 352–363. [CrossRef]
146. Rao, S.I.; Woodward, C.; Parthasarathy, T.A.; Senkov, O. Atomistic simulations of dislocation behavior in a model FCC multicomponent concentrated solid solution alloy. *Acta Mater.* **2017**, *134*, 188–194. [CrossRef]
147. Zhao, X.; Wang, Y.; Song, X.; Wang, Y.; Chen, Z. Segregation behavior of alloying elements and its effects on stacking fault of γ' phase in Ni-based superalloys: First-principles study. *Comput. Mater. Sci.* **2022**, *202*, 110990. [CrossRef]
148. Feng, W.; Qi, Y.; Wang, S. Effects of Short-Range Order on the Magnetic and Mechanical Properties of FeCoNi(AlSi)x High Entropy Alloys. *Metals* **2017**, *7*, 482. [CrossRef]
149. Wang, J.; Jiang, P.; Yuan, F.; Wu, X. Chemical medium-range order in a medium-entropy alloy. *Nat. Commun.* **2022**, *13*, 1021. [CrossRef]
150. Su, Z.; Ding, J.; Song, M.; Jiang, L.; Shi, T.; Li, Z.; Wang, S.; Gao, F.; Yun, D.; Ma, E. Enhancing the radiation tolerance of high-entropy alloys via solute-promoted chemical heterogeneities. *Acta Mater.* **2023**, *245*, 118662. [CrossRef]
151. Dobbelstein, H.; Gurevich, E.L.; George, E.P.; Ostendorf, A.; Laplanche, G. Laser metal deposition of compositionally graded TiZrNbTa refractory high-entropy alloys using elemental powder blends. *Addit. Manuf.* **2019**, *25*, 252–262. [CrossRef]
152. Lu, K. Making strong nanomaterials ductile with gradients. *Science* **2014**, *345*, 1455–1456. [CrossRef] [PubMed]
153. Ma, E.; Zhu, T. Towards strength–ductility synergy through the design of heterogeneous nanostructures in metals. *Mater. Today* **2017**, *20*, 323–331. [CrossRef]
154. Wang, Y.M.; Voisin, T.; McKeown, J.T.; Ye, J.; Calta, N.P.; Li, Z.; Zeng, Z.; Zhang, Y.; Chen, W.; Roehling, T.T. Additively manufactured hierarchical stainless steels with high strength and ductility. *Nat. Mater.* **2018**, *17*, 63–71. [CrossRef] [PubMed]
155. Zhu, J.; Sun, L.; Bie, Z.; Tian, X.; He, X. Tailored tensile properties of CoCrNi medium entropy alloy by tuning the elemental distribution. *J. Alloy. Compd.* **2022**, *897*, 163171. [CrossRef]
156. Zhu, J.; Sun, L.; Li, D.; Zhu, L.; He, X. Compositional undulation induced strain hardening and delocalization in multi-principal element alloys. *Int. J. Mech. Sci.* **2023**, *241*, 107931. [CrossRef]
157. Chen, Y.; Fang, Y.; Wang, R.; Tang, Y.; Bai, S.; Yu, Q. Achieving high strength and ductility in high-entropy alloys via spinodal decomposition-induced compositional heterogeneity. *J. Mater. Sci. Technol.* **2023**, *141*, 149–154. [CrossRef]
158. Wu, H.; Huang, M.; Li, Q.; Wu, J.; Li, J.; Wang, Z.; Fan, G. Manipulating the plastic strain delocalization through ultra-thinned hierarchical design for strength-ductility synergy. *Scr. Mater.* **2019**, *172*, 165–170. [CrossRef]
159. Hofmann, D.C.; Kolodziejska, J.; Roberts, S.; Otis, R.; Dillon, R.P.; Suh, J.-O.; Liu, Z.-K.; Borgonia, J.-P. Compositionally graded metals: A new frontier of additive manufacturing. *J. Mater. Res.* **2014**, *29*, 1899–1910. [CrossRef]